Low strain variation design method of the quadrupolar fiber coil based on the comprehensive stress analysis

LIANJIE SHAN[a,b], JING LI[b], JUNLI LIU[c], HAO SU[c], YINGCHUN LIANG[a]
[a]*School of Mechatronics Engineering, Harbin Institute of Technology, Harbin 150001, China*
[b]*Beijing Aerospace Times Optical-electronic Technology Co. Ltd., Chinese Academy of Aerospace Electronics Technology, Beijing 100094, China*
[c]*Beijing Institute of Aerospace Control Device, Beijing 100039, China*

As a sensitive element of the fiber optic gyroscope (FOG), the fiber coil has a significant effect on the accuracy of FOG. The performance of the fiber coil is severely influenced by the internal strain caused by the winding process. In this paper, a new design method is proposed by studying the stress in a quadrupole wound fiber gyro coil comprehensively in order to decrease the strain variation in the fiber coil, which is the low strain design method. Based on the proposed method, the tension stress, the bend-induced stress and the curing stress in the fiber coil during the manufacturing process is studied. Then, the qualified fiber coil for the FOG is obtained by the low strain design method. At last, the experimental results show that the proposed method can effectively reduce the internal strain variation in the fiber coil, which ensures the FOG a good temperature and vibration performance.

(Received April 26, 2016; accepted June 7, 2017)

Keywords: Fiber optic gyroscope, Fiber coil, Stress, Strain

1. Introduction

Fiber coil is the key component of FOG to realize Sagnac effect, which includes flange-supported fiber coil and freestanding fiber coil. For the flange-supported fiber coil the fiber coil is wound tightly at the external surface of frame. However, for the freestanding fiber coil, the fiber coil is wound on a detachable frame which is removed after winding. With the characteristic of stress-sensitivity, the optical fiber which is restraint by the frame will cause the large non-reciprocal error. Then, without the influence of the frame, the internal stress of the optical fiber in the freestanding fiber coil is much lower than that in the flange-supported fiber coil. Therefore, in order to improve the long-term bias stability of the FOG, the freestanding fiber coil is used widely in the high-precision case. In addition, more and more attention has been focused on the research of the freestanding fiber coil. Chen et al. studied the influence of gluing process on the performance of freestanding fiber coil and FOG [1], which arrived at the conclusion that uniform gluing with slow curing process is benefit for the precision improvement of FOG. Meng and Chen et al. studied the performance of the freestanding fiber coil with different types of adhesives [2,3]. The results show that suitable adhesives are helpful to the performance improvement of freestanding fiber coil. Meanwhile, the types of adhesives can not only affect the performance of the freestanding fiber coil, but also can lead to fiber breakage sometimes. Meng et al. analyzed the stresses in the freestanding fiber coil during winding process and demonstrated that the stress control during winding process is essential to the quality of the fiber coil [4]. However, previous studies are mainly focused on the measurement of the internal strain in the fiber coil, the winding tension equipment, and the curing stress of the fiber coil, which cannot provide theoretical basis for the design of the fiber coil. Therefore, the design method of the fiber coil should be studied in order to ensure the performance of the FOG.

In this paper, the low strain design method of the fiber coil is proposed based on the comprehensive stress analysis. Stresses and corresponding influencing factors in the fiber coil are first analyzed and optimal design methods are demonstrated to reduce the stresses in the fiber coil. The optimized fiber coil is then verified and the test results show that the performance of the fiber coil has a great improvement with a better uniformity.

2. Stress analysis of the fiber coil

The freestanding fiber coil consists of optical fiber and the adhesive which uniformly surrounds the optical fiber. Fig. 1 shows the diagram of the freestanding fiber coil.

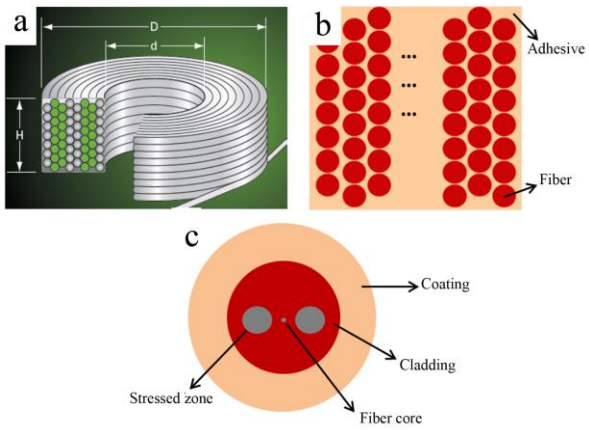

Fig. 1. Freestanding fiber coil (a) structural diagram (b) cross section diagram (c) cross section of fiber

The performance of the fiber coil is influenced directly by the internal strain change which will result in the refractive index change of the optical fiber. Then, the phase and amplitude of the propagating light in the fiber is changed, which will cause the phase shift of the FOG output, as shown in Eq. (1) [5].

$$\Delta\phi_E(t) \approx \frac{\beta}{v}\frac{dn}{d\varepsilon}\int_0^L \frac{d\varepsilon}{dt}(z,t)(L-2z)]dz \qquad (1)$$

Where β is the propagation constant, v is the light speed, ε is the fiber strain, L is the length of fiber coil, z is a point in the fiber coil.

In the Eq. (1), the fiber strain ε is caused by the external stress which the optical fiber is very sensitive to. Because the optical fiber is a kind of elastic medium, the stress of the optical fiber is linearly proportional to its stain, which is given by

$$\sigma = \varepsilon \cdot E \qquad (2)$$

In which, σ is the stress in the fiber coil that expresses the force per unit area, Pa, E is the Young's modulus, 72 GPa.

According to Eq. (1)-(2), the accuracy of the fiber coil can be improved by reducing the external stress in the fiber coil. Therefore, in order to propose the reasonable design method, the external stress in the fiber coil is studied firstly.

During the winding process of the fiber coil, the tension stress, the bend-induced stress and the curing stress are caused by the winding tension, the round frame and the glue, respectively. In addition, the thermal stress will also occur with the change of the ambient temperature. In the fiber coil, all the four types of stress add together, which will influence the performance of the fiber coil. Therefore, all the four types of stress in the fiber are studied as followed.

2.1. Tension stress analysis

In the fiber coil, the optic fiber is wound under certain winding tension which is 3g to 20g. The winding tension will cause the tension stress which is given by Eq. (3).

$$\sigma_F = \frac{Fg}{1000\pi r_{th}^2} \qquad (3)$$

Where r_{th} is the radium of optical fiber, σ_F is the tension stress and the Fg is the external winding tension.

For the fiber coil, the large winding tension ensures a neatly arrangement of the optical fiber. However, the larger the winding tension is, the greater the tension stress is. On the contrary, applying a small winding tension can reduce the internal tension stress, but it increases the difficulty to control the tension and decreases the tension stability, which is not good for maintaining the symmetry of the fiber coil. Therefore, the tension stress in the fiber coil should be controlled.

2.2. Bend-induced stress analysis

In order to obtain the bend-induced stress in the fiber coil, the structure of the optical fiber in the fiber coil is studied, as shown in Fig. 2.

Fig. 2. Structure of the optical fiber in the fiber coil

In the optical fiber, the bend-induced stress distribution is not uniform. As shown in Fig. 2, the surface at the A side of the fiber suffers from tensile stress and the surface at the B side of the fiber suffers from compressive stress. Meanwhile, the maximum strain appears at the position of point A, which is given by

$$\varepsilon_{\max} = \frac{r}{R + r + C_{th}} \qquad (4)$$

Where r is the radius of the fiber cladding, R is the bending radius, C_{th} is the thickness of the fiber coating. Because $R \gg r + C_{th}$, the equation (4) can be the simplified to Eq. (5).

$$\varepsilon_{\max} = \frac{r}{R} \qquad (5)$$

Then the maximum bend-induced stress is given by Eq. (6).

$$\sigma_{\max} = \frac{E \cdot r}{R} \tag{6}$$

As shown in Fig. 1, the bending tension at the point of B is given by Eq. (7).

$$\sigma_b = \sigma_{\max} \sin\theta = \frac{E \cdot r}{R} \sin\theta \tag{7}$$

According to Eq. (5)-(7), the smaller the radius of the fiber coil is, the larger the bending tension is. Therefore, the bend-induced stress can be controlled by reducing the radius of the fiber coil.

In addition, there are also micro bends in the fiber coil, which lead to severe strain. As shown in Fig. 3, the micro bend occurs when the fiber shifts from one layer to another layer with a bending radius from 20 mm to 80 mm. In order to improve the accuracy of the fiber coil, the micro bend should also be controlled.

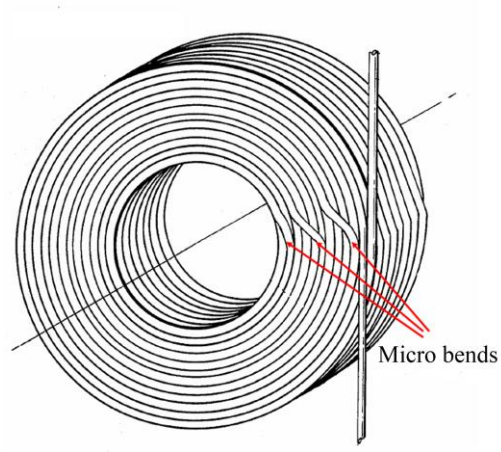

Fig. 3. Micro bends in the fiber coil

2.3. Curing stress analysis

The volume of the adhesive shrinks during the curing process, so the curing stress occurs in the fiber coil, which is given by Eq. (8).

$$\sigma_s = \alpha_s \cdot E + \alpha_T \cdot E \cdot \Delta T \tag{8}$$

Where α_s is the volume shrinkage of the adhesive and E is the fiber modulus, α_T is the thermal expansion coefficient of the glue, ΔT is the temperature variation during the curing process. According to the expression, the curing stress mainly depends on the shrinkage of the adhesive. Therefore, the curing stress can be reduced by applying the adhesive with small shrinkage [6-7].

2.4. The stress analysis

Based on the stress analysis, the stresses in a fiber coil mainly include the tension stress, the bend-induced stress, the curing stress and the thermal stress, which is given by Eq. (9).

$$\sigma = \sigma_F + \sigma_b + \sigma_s = \frac{Fg}{1000\pi r_{th}^2} + \frac{E \cdot r}{R} \cdot \sin\theta + \alpha_s \cdot E + \alpha_T \cdot E \cdot \Delta T \tag{9}$$

According to Eq. (9), the key factors that influence the stress of the fiber coil are the winding tension, the bending radius and the shrinkage. Then the influence of the key factors on the stress of the fiber coil is obtained by the simulation, as shown in Fig. 4.

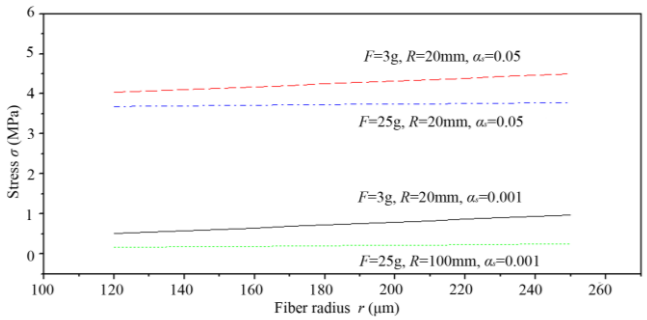

Fig. 4. Simulation results of the internal strain with different fiber parameters

As shown in Fig. 4, the stress in the fiber coil is influenced greatly by the key factors which should be optimized by the reasonable method in order to improve the performance of the fiber coil. Therefore, the low strain variation design method is proposed for the fiber coil.

3. Low strain variation design method of the fiber coil

Based on the stress analysis, the low strain variation design method of the fiber coil is proposed, the schematic diagram of which is shown in Fig. 5.

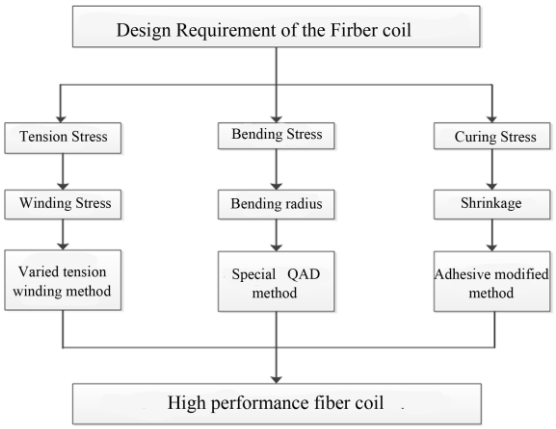

Fig. 5. Schematic diagram of the low strain variation design method

As shown in Fig. 5, the low strain variation design method consists of three methods, which are the varied tension winding method, the special quadrupole symmetric winding method and the adhesive modification method. In the low strain method, the winding stress, the bend-induced stress and the curing stress are reduced by the varied tension winding method, the special quadrupole symmetric winding method and the adhesive modification method, respectively. In order to state the low strain variation design method clearly, all the three methods are explained as followed.

3.1. Varied tension winding method

For practical coil winding, the frame needs to be pretreated in order to match its thermal expansion coefficient with the optical fiber. After pretreatment, the surface hardness of the frame is lower than the hardness of optical fiber. When the fiber coil is wound with equivalent tension, the stresses of the fibers at the bottom layers can be mostly released. With the increase of the winding layers, the stresses of the fibers at the top layers are hard to release. This leads to smaller residual stress at the bottom layer and larger residual stress at the top layer. For limiting case, the residual stress difference between the top layer and bottom layer can be as large as the stress caused by the winding tension. The largest stress difference can be calculated by Eq. (10). However, the practical value will be smaller than this largest value.

$$\frac{F}{\pi r^2} = \frac{T\cos\theta}{\pi r^2} = \varepsilon E \qquad (10)$$

where, F is the force along the fiber axis, T is the tensile force during winding process, θ is the angle between F and T, lower the surface hardness of the frame bigger θ, r is the fiber radius, ε is the strain in the fiber, E is the modulus of the fiber.

In order to make the stress distribute uniformly in the fiber coil, different winding tensions should be applied for different fiber layers according to the residual stress, especially for the bottom layers near the frame.

Therefore, the varied tension winding method is proposed, which is composed of three steps.

1) Firstly, according to the fiber diameter, the fiber type, the frame diameter and the frame material, the pre-winding experiment is carried out, by which the strain distribution curve is obtained.

2) Secondly, Based on the strain distribution curve, the difference of the stress among the different layer is calculated according to Eq. (10), by which the tension table of the different layers is obtained.

Take a fiber coil wound with 10g tension for instance, the strain variation is larger for the layers near the frame. For the first four layers, as shown in Fig. 6, the first layer has a smaller strain with an average value of 175 με. The strain increases with the layers, the fourth layer has an average strain of 260με. Assume the fiber diameter is 0.168 mm, the cladding radius is 0.04mm, and the modulus is 72Gpa, the strain caused by 10g tension is around 270με. In order to make the strain in each layer reaches a level of 270με, the winding tension needs to be increased. Table 1 shows the relation of tension value and winding layers.

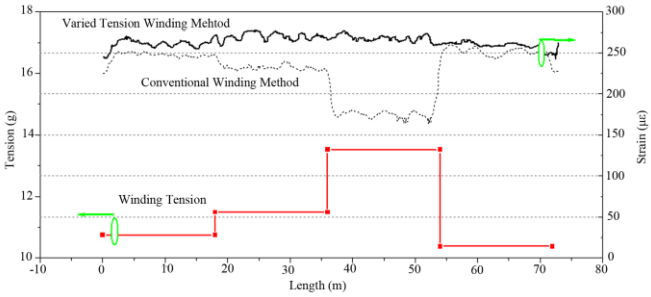

Fig. 6. The strain distributions of the fiber coil with different winding methods

Table 1. Tension applied for different fiber layers with varied tension method

Layer	Strain for conventional winding method (με)	Tension for the varied tension method (g)
1	175	13.5
2	230	11.5
3	250	10.7
4	260	10.4

3) Finally, the fiber coil is wound according to the tension table.

In order to validate the varied tension winding method, the experiment is carried out, by which the strain distributions of the fiber coils obtained by the varied tension winding method and the conventional winding method are measured. The experimental results and the winding tension used in the varied tension winding method are shown in Fig. 6.

As shown in Fig. 6, the winding tension used in the varied tension winding method changes from 0g to 4g. By the varied tension winding method, variation of the winding stress in the fiber coil is reduced effectively.

3.2. Special quadrupole symmetric winding method

During the winding process, the fiber is wound on the frame under certain tension, as shown in Fig. 7.

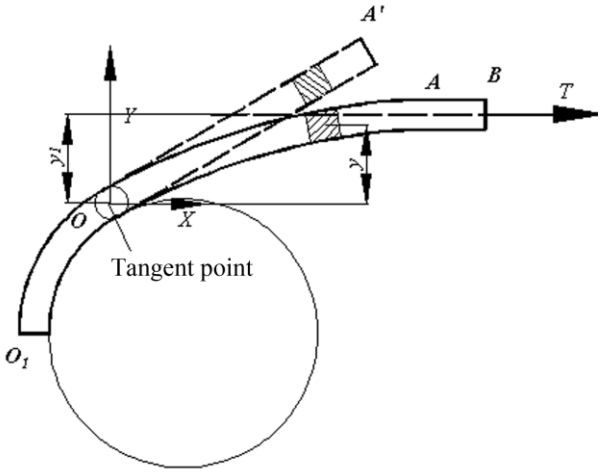

Fig. 7. The winding diagram of optical fiber

For the fiber coil, the conventional quadrupole symmetric winding (QAD) method is shown in Fig. 8.

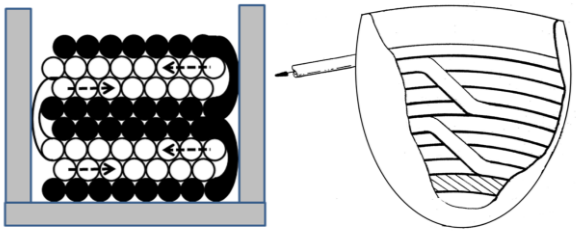

Fig. 8. The conventional QAD method

For conventional QAD method, in order to keep the quadrupole symmetry at the layer shifting position, the bottom layer fiber needs to cross two fiber layers. When the fiber shifts the layer, the sharp decrease of the fiber bending radius leads to the huge variation of the tension in the fiber; while after the layer shift, the bending radium increases, the variation is two times of the fiber diameter. Compared with the frame, it can be approximately considered that the bending radius and tension of the fiber recover to the level before the layer shift. The tension variation during the layer shifting process results in the stress variation of the fiber. Equation 11 gives the relation of bending radius and tension of a point in the fiber:

$$y = \frac{EI}{RT}\left(1 - e^{-x\sqrt{\frac{T}{EI}}}\right) \tag{11}$$

In which, x and y are the coordinate values of a point in the fiber, E is the modulus of fiber coil, R is the bending radius, I is polar moment of inertia relative to the fiber center, and T is the winding tension of the fiber. Equation 11 indicates that the coordinate of certain point in the fiber has corresponding relations with the bending radius and the winding tension.

Therefore, special quadrupole symmetric winding method is proposed to solve this problem, as shown in Fig. 9.

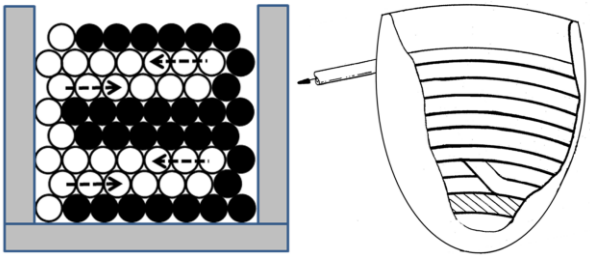

Fig. 9. The special QAD method

Compared with the conventional QAD method, the fiber will not be squeezed when shifting layers and the bending radius for each layer is almost the same by applying special QAD method. The fiber can be smoothly transited from the inner layer to the outer layer by the special QAD method, which can effectively avoid the lateral squeeze.

3.3. Adhesive modification method

According to the curing mechanism, the distance between adhesive molecules changes from van der Waals range to covalent bond range during the curing process, that is almost from 0.3~0.5nm to 0.154nm. The atom arrangement in polymer is much tighter than that before curing. This leads to the volume shrinkage during the curing and causes the strain in the fiber increase. Fig. 10 shows the diagram of curing process.

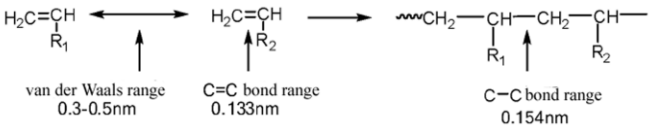

Fig. 10. The range change of adhesive atoms during curing process

In order to decrease the shrinkage of the adhesive, adding inorganic nano materials into the adhesive is an effective approach. Since the inorganic nano materials will not participate in the curing process, the volume percentage of the adhesive is reduced by adding the inorganic material. So, the shrinkage gets decreased [8-10]. The curing process of the adhesive, ET-1, after adding inorganic material is shown in Fig. 11. The added materials will also evidently improve the thermal expansion coefficient and thermal conductivity.

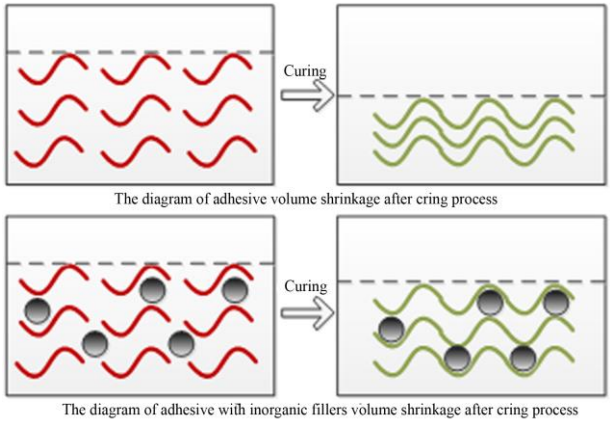

Fig. 11. The curing diagram of the adhesive before and after adding inorganic materials

Choose SiO_2 as the adding material will decrease the shrinkage of the adhesive, Moreover, due to the high thermal conductivity of SiO_2, the thermal conductivity of the adhesive could be improved as well by adding SiO_2. The diameter of the SiO_2 particle is chosen as 20nm since larger particles have the risk to break the fiber and even cause fiber fracture. The SiO_2 particles are mixed with adhesive via mechanical ultrasonic resonance method, and the adhesive/SiO_2 mixture can be obtained with different mixing ratios.

In order to validate the adhesive modification method, the experiment is carried out. The curing shrinkage and viscosity of the adhesives with different mass fraction of the nano silica particles is shown in Fig. 12.

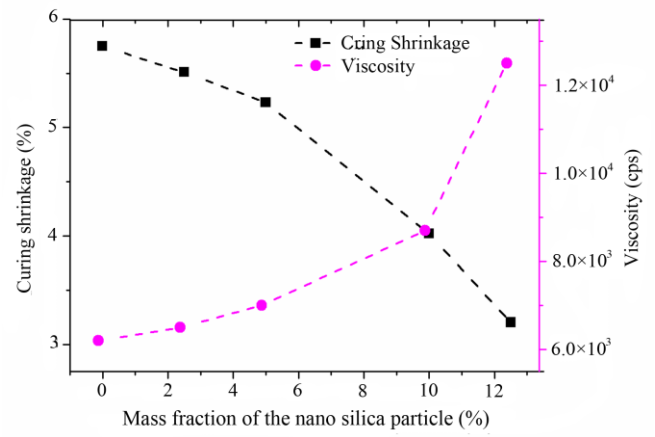

Fig. 12. The curing diagram of the adhesive before and after adding the inorganic particles

As shown in Fig. 12, with the increase of SiO_2, the curing shrinkage of the adhesive decreases and the viscosity increases. The shrinkage of the adhesive is reduced by 30% when the mass fraction reaches 10%, which validates the adhesive modification method. Although the shrinkage can keep decreasing when keep increasing the percentage of SiO_2, the viscosity of the adhesive increases severely. This makes the adhesive not suitable for fiber coil fabrication any more. Therefore, the percentage of SiO_2 is chosen as 10%.

4. Experiment verification

Applying the varied tension winding method, the special QAD winding method and the modified adhesive method is not difficult to practical fabrication. Fig. 13 shows the fiber coil products fabricated with the optimized methods.

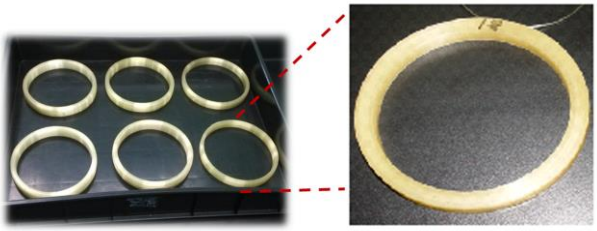

Fig. 13. Fiber coils wound with optimized method

Meanwhile, the strain distribution in the fiber measured with AQ8603 after optimizing is shown in Fig. 14, which becomes more uniform. Before optimizing, the strain distribution shows large variation with sudden changes at the layer shift positions. The peak-peak value of the strain is 150με within the whole length of fiber coil; while after optimizing the fiber coil, the peak-peak value decreases to 50με with no sudden changes at the layer shift positions. Because of the smaller curing shrinkage of the adhesive, the strain is becoming smaller too.

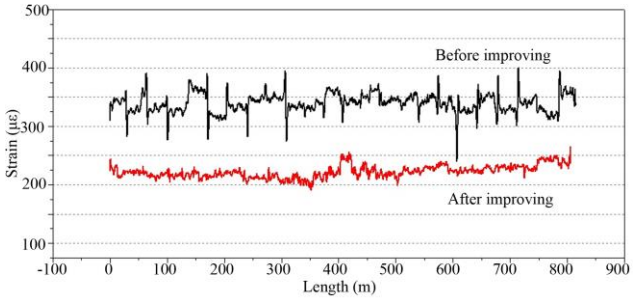

Fig. 14. Strain distribution in fiber coil before and after optimizing

FOG temperature performance test was conducted with 30 fiber coils before optimizing and 30 fiber coils after optimizing, respectively. The temperature range is -40 °C～60 °C with a gradient of 1 °C /min. As shown in Fig. 15, for the fiber coils before optimizing, the peak-peak values of FOG output are mainly within the

range of 0.9～1.6 °/h; While for the fiber coils after optimizing, the peak-peak values of FOG output are mainly smaller than 1.0 °/h. The experimental results have validated the varied tension winding method, the special QAD winding method and the adhesive modification method. By combining the optimizing methods together, the temperature performance of the FOG is improved by 37%.

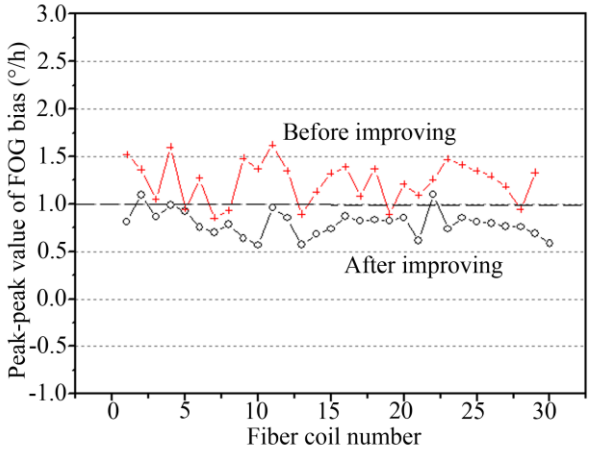

Fig. 15. Temperature performance of FOG before and after optimizing the fiber coil

5. Conclusion

In this paper, the low strain variation method is proposed to improve the performance of the fiber coil based on the comprehensive stress analysis, which is composed of the varied tension winding method, the special quadrupole symmetric winding method and the adhesive modification method. The low strain variation method lays the foundation for the design of the fiber coil. At last, the low strain variation method is validated by the experiment, the temperature performance of FOG is improved by 37%, which has an important significance to the development of the FOG.

References

[1] Chen Jun, Wang Wei, Li Jing, Zhao Zhengxin, Journal of Chinese Inertial Technology 109 (2012).
[2] Meng Zhaokui, Shao Hongfeng, Xu Hongjie, Zhang Chunxi, Journal of Beijing University of Aeronautics and Astronautics **32**(8), 958 (2006).
[3] Chen Xiaojun, Zhu Yiqing, Xu Jiancai, et. al., Optical Fiber & Electric Cable **5**(5), 24 (2012).
[4] Meng Zhaokui, Zhang Chunxi, Yang Yuanhong, Journal of Beijing University of Aeronautics and Astronautics **31**(3), 307 (2005).
[5] F. Mohr, F. Schadt, Second European Workshop on Optical Fibre Sensors, Proceedings of SPIE **5502**, 410 (2004).
[6] Zhao Xin, Yu Yu, Wu Jianwei, Chemistry and Adhesion **30**(3), 24 (2008).
[7] Zhou Xiaoyan, Jiang Ling, New Chemical Materials **31**(7), 20 (2003).
[8] Frank Bauer, et al., Macromolecular Chemistry and Physics **201**(18), 2654 (2000).
[9] Frank Bauer, et al., Macromolecular Chemistry and Physics **204**(3), 375 (2003).
[10] Frank Bauer, et al., Macromolecular Materials and Engineering **287**(8), 546 (2002).

*Corresponding author: 13401128255@163.com